Self-avoiding polymer trapped inside a cylindrical pore: Flory free energy and unexpected dynamics

Youngkyun Jung*
Supercomputing Center, Korea Institute of Science and Technology Information, P.O. Box 122, Yuseong-gu, Daejeon 305-806, Korea

Suckjoon Jun†
FAS Center for Systems Biology, Harvard University, 52 Oxford Street, Cambridge, Massachusetts 02138, USA

Bae-Yeun Ha‡
Department of Physics and Astronomy, University of Waterloo, Waterloo, Ontario, Canada N2L 3G1
(Received 19 December 2008; published 9 June 2009)

We study the elastic and dynamic behavior of a self-avoiding chain confined inside a cylindrical pore using a Flory-type approach and molecular-dynamics simulations. In the Hookean regime, we find that the effective spring constant of the chain is given by $k_{\mathrm{eff}} \sim N^{-1} D^{-\gamma}$, where N is the number of monomers and D the diameter of the pore. While the Flory approach reproduces the earlier scaling result $\gamma = 1/3$, our simulations confirm a more recent numerical result $\gamma \approx 0.9$ for the computationally accessible regimes. In the absence of hydrodynamic interactions, the relaxation dynamics of a stretched-and-released chain in this regime is characterized by a global relaxation time $\tau_R \sim N^2 D^{\gamma}$ with the same exponent γ for k_{eff}. We also discuss how chain relaxation under confinement is influenced by hydrodynamic interactions. In the presence (or absence) of the hydrodynamic interaction, the finite-size effect observed in k_{eff} is shown to persist in chain relaxation, resulting in τ_R markedly different from previous results.

DOI: 10.1103/PhysRevE.79.061912 PACS number(s): 87.15.−v, 82.35.Lr, 82.37.Rs

I. INTRODUCTION

Confinement influences the equilibrium and dynamic properties of a polymer in a fundamental way. Reptation is a well-known example, where the basic length and time scales of chain molecules are altered qualitatively because of a tubelike spatial constraint each chain experiences [1,2]. In a living cell, many essential physical processes involving biopolymers, from protein translocation [3] to bacterial chromosome segregations [4], may have evolved in a specific way because of the presence of various spatial confinements in the cell. On the other hand, nanofabrication technologies have allowed one to probe the elastic properties of double-stranded DNA in both pore- and slitlike geometries, especially when the confining dimension is comparable to the persistence length of the strands [5,6]. In the context of polymer thin films, the role of confinement on glass transitions has been extensively discussed [7]. Despite its fundamental and practical importance, theoretical understanding of chain molecules in a pore has remained far behind the experimental progress. We have recently reported force-deformation relations of such a chain [8], but we did not explore its implications on dynamics.

The main purpose of this paper is to present a quantitative picture of the elastic and dynamical properties of a cylindrically confined polymer. As we shall discuss, these two properties are closely related to and complement each other, especially when hydrodynamic effects can be ignored. To this end, we bring together a Flory-type approach and molecular-dynamics (MD) simulations. Moreover, to address the significance of hydrodynamic interactions in determining chain relaxation, we combine our simulation results and a theoretical approach to chain diffusion in a pore developed by Harden and Doi [9].

We first show that in the absence of hydrodynamic interactions our Flory approach is fully consistent with the scaling approach by Brochard and de Gennes [10]; it correctly reproduces the scaling results for confinement free energy and global relaxation times τ_R, among others. On the other hand, our numerical results for τ_R, in the presence or absence of hydrodynamic interactions, noticeably differ from those found in previous simulation studies [11,12], which support the scaling predictions [10] [see Eq. (6)]. They are, however, consistent with more recent simulations that clearly suggest *un*expected relaxation of chain molecules trapped in a cylindrical pore in the computationally accessible regimes [8,13] (as already hinted much earlier by Kremer and Binder [14]). To see this effect, in the presence of hydrodynamic interactions, we calculate chain friction ξ_{chain} (thus τ_R as well) by explicitly using our simulation data in the aforementioned approach [9]. This enables us to track down the origin of the discrepancy: the main cause is the finite-size effect extensively discussed recently [13], which persists in chain relaxation (whether the hydrodynamic interaction is included or not).

This paper is organized as follows. In Sec. II, we present a (renormalized) Flory theory of a self-avoiding chain trapped in a cylindrical pore with a brief discussion on a corresponding problem in slit geometry. Simulation methods and results for τ_R are discussed in Sec. III, followed by our analysis on hydrodynamic interactions and finite-size effects.

*yjung@kisti.re.kr
†sjun@cgr.harvard.edu
‡byha@uwaterloo.ca

II. FLORY THEORY

A. Cylindrical confinement

Much progress in understanding chain molecules often thrives on simplification due to their intrinsic complexity. In this regard, it is hard to exaggerate the success and impact of Flory's brilliant scheme for computing the equilibrium size of a swollen polymer chain in a good solvent [15].

Consider a swollen polymer carrying N monomers of size a each with its end-to-end distance R. Then, the *trial* Flory free energy in d spatial dimensions is expressed as [16]

$$\beta\mathcal{F}_d(R) \sim \frac{R^2}{Na^2} + \frac{a^d N^2}{R^d}. \tag{1}$$

Here and below, $\beta=1/k_BT$ with k_B as the Boltzmann constant and T as the absolute temperature. Also, we only consider an *athermal* case, i.e., the excluded volume of each monomer is a^d independent of T. The first term describes the chain elasticity of an "entropic spring," while the second term represents the mean-field energy of (two-body) excluded-volume interactions between monomers on the chain [1,15]. The equilibrium chain size or the Flory radius, R_F, is obtained by minimizing $\mathcal{F}_d$ with respect to R: for $d\leq 4$, $R_F\sim aN^\nu$ with $\nu=3/(2+d)$ (e.g., $\nu=3/5$ for $d=3$). This exponent ν is rightly designated as the Flory exponent.

As de Gennes correctly pointed out, however, Flory's theory benefits from the "remarkable cancellation" of errors (overestimates) of both terms in Eq. (1) [1]. To see this, note that at $R=R_F$ the Flory free energy scales as

$$\beta\mathcal{F}_d(R_F) \sim N^{(4-d)/(2+d)}. \tag{2}$$

This is equivalent to stating that the number of monomer contacts scales as $N^2/R_F^d \sim N^{2-\nu d}$ ($\sim N^{1/5}$ for $d=3$ [17]), consistent with the mean-field theory. For $d=3$, however, this is an overestimate and, in fact, $\beta\mathcal{F}_{d=4}(R_F)\sim 1$ is expected to be asymptotically valid in $d=3$ [18–21].

Despite the aforementioned limitations, mainly due to its simplicity, Flory-type approaches have been extended to many other important cases, e.g., linear chains with stiffness [22,23] and polymers of various topology in a confined space (for a review, see Ref. [24]). In particular, the widely used free energy of a linear chain in a cylindrical pore has the following form [24,25]:

$$\beta\mathcal{F}(R_\parallel, D) \sim \frac{R_\parallel^2}{Na^2} + \frac{a^3N^2}{D^2R_\parallel}, \tag{3}$$

where $R_\parallel$ is the trial chain size in the longitudinal direction and D is the width of the cylinder (see Fig. 1).

Although Eq. (3) produces the correct scaling for the equilibrium chain size $R_{\parallel 0}\sim Na(a/D)^{2/3}$ [1], its applicability beyond the computation of $R_{\parallel 0}$ is limited by the following two important errors: (i) for a chain in equilibrium ($R_\parallel=R_{\parallel 0}$), Eq. (3) predicts $\beta\mathcal{F}\sim N(a/D)^{4/3}$, but the correct free energy should scale as $\beta\mathcal{F}\sim N(a/D)^{5/3}$ [1,10]. (ii) Equation (3) results in an effective "Hookean" spring constant $k_{\rm eff}$ of the chain, given by $\beta k_{\rm eff}=(\partial^2\beta\mathcal{F}/\partial R_\parallel^2)_{R_\parallel=R_{\parallel 0}}\sim N^{-1}a^{-2}$, but the standard scaling result is $\beta k_{\rm eff}\sim N^{-1}D^{-1/3}a^{-5/3}$ [6,10]. These drawbacks share the same origin as the Eq. (2) for $d=3$ by breaking the "k_BT per blob" ansatz.

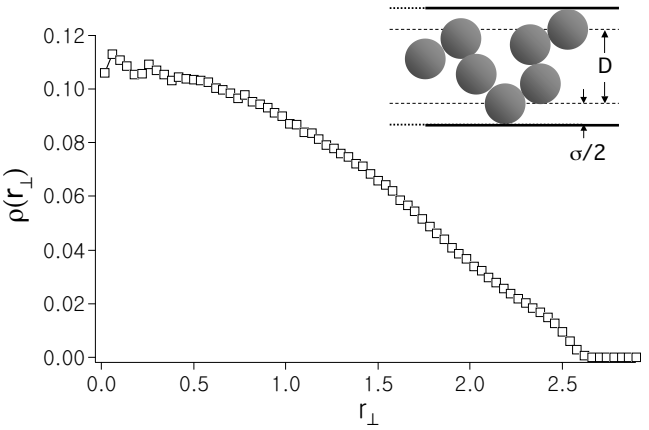

FIG. 1. MD simulation results (squares) for the normalized density of monomers, $\rho(r_\perp)$, for $N=256$ and $D=5$, as a function of $r_\perp$, the normal distance from the symmetry axis of the cylinder in units of σ. Because of the wall effect, $\rho(r_\perp)$ decays to zero as $r_\perp$ approaches the radius of the cylinder, $R_\perp=D/2$. Here the diameter D is roughly the maximum normal distance between the centers of two monomers, as illustrated in the inset.

Recently, we have proposed, and confirmed using simulations, the following "renormalized" free energy for a polymer under cylindrical confinement near its equilibrium length [8],

$$\beta\mathcal{F}_{\rm cyl}(R_\parallel, D) \sim \frac{R_\parallel^2}{(N/g)D^2} + \frac{D(N/g)^2}{R_\parallel}, \tag{4}$$

where g is the number of monomers inside a blob of diameter D, i.e., $g\simeq(D/a)^{5/3}$. The basic idea is to consider the confined space inside a cylinder as an effective one-dimensional space ($d=1$) and, hence, to introduce the length scale D accordingly in Eq. (1) by rescaling $a\to a'=D$ and $N\to N'=N/g$. Then, the first term can be understood as the chain being made of N/g subunits ("blobs") of size D, while the second term describes the mutual exclusion between neighboring blobs.

Indeed, the above free energy produces not only the expected equilibrium chain size $R_{\parallel 0}\sim Na(a/D)^{2/3}$, but also the correct blob-overlapping free energy of $\beta\mathcal{F}_{\rm conf}\sim N/g \sim N(a/D)^{5/3}$ (namely, the total number of blobs) [1,10]. Note that this is identical to the earlier result for confinement free energy based on the blob-scaling approach [1]. Importantly, we obtain the correct effective Hookean spring constant of the chain: $k_{\rm eff}\sim\partial^2\mathcal{F}_{\rm cyl}/\partial R_\parallel^2|_{R_\parallel=R_{\parallel 0}}\sim N^{-1}a^{-1/\nu}D^{1/\nu-2} \sim N^{-1}a^{-2}(a/D)^{1/3}$ [6,10]. Moreover, using the stretch-release argument, the global (slowest) relaxation time of the confined chain (in the absence of hydrodynamic effects) is then reciprocally obtained as $\tau_R\sim N/k_{\rm eff}\sim N^2a^{1/\nu}D^{2-1/\nu} \sim N^2a^2(D/a)^{1/3}$, consistent with the earlier scaling result [6,10].

B. Slit geometry

A natural extension of Eq. (4) to the slit case [26] would be obtained from Eq. (1) with the same rescaling of $a \to a' = D$ and $N \to N' = N/g$, assuming $d=2$, as follows:

$$\beta \mathcal{F}_{\text{slit}}(R_{\|}, D) \sim \frac{R_{\|}^2}{(N/g)D^2} + \frac{D^2(N/g)^2}{R_{\|}^2}, \tag{5}$$

where D is the distance between the two parallel slits and $g \sim (D/a)^{5/3}$. Indeed, this free energy predicts the correct equilibrium size of the chain in a slit, $R_{\|0} \sim aN^{3/4}(a/D)^{1/4}$, in agreement with the results of other approaches [1,24]. However, its equilibrium free energy, $\beta \mathcal{F}_{\text{slit}}(R_{\|}=R_{\|0}, D)$, scales as $N^{1/2}(a/D)^{5/3}$. Note that this is different from the free energy of slit confinement $\beta \mathcal{F}_{\text{conf}} \sim N/g \sim N(a/D)^{5/3}$, which is identical to that of a cylinder up to numerical prefactors (see Refs. [1,26] and references therein). Beyond the computation of $R_{\|0}$, the applicability of the slit free energy in Eq. (5) is questionable.

Why does the Flory approach work better for the cylinder case than for higher dimensions? To see the difference, consider the volume fraction (α) of monomers inside a space explored by a self-avoiding chain in equilibrium. For cylindrical confinement, this is given by $\alpha = Na^3/D^2R_{\|0} \sim (D/a)^{-4/3}$, *independent* of N, whereas, both for a slit and for a dilute bulk solution, $\alpha \to 0$ as $N \to \infty$. It is this special nature of compactness of one-dimensional space that explains the extensiveness and thus the success of the rescaled Flory approach in Eq. (4) [27].

III. SIMULATIONS AND RESULTS

A. Simulation methods

We have conducted MD simulations with a bead-spring model of polymers trapped inside a cylindrical pore. Beads or monomers (among themselves and with the confining walls) interact via the fully repulsive Weeks-Chandler-Andersen (WCA) potential [28], $U_{\text{WCA}}(r) = 4\epsilon[(r/\sigma)^{-12} - (r/\sigma)^{-6} + 1/4]$ for $r < 2^{1/6}\sigma$ and 0 otherwise. Here, ϵ and σ represent the strength and range of the WCA potential, respectively. (Accordingly, $\sigma \simeq a$ in our simulations.) Finally, r denotes the center-to-center distance between two beads, or the distance of a bead center from the confining cylinder minus σ; as a result, the diameter D is the maximum distance normal to the cylinder between the centers of two beads (see the inset of Fig. 1).

The bond between two neighboring beads was modeled by the finite extensible nonlinear elastic potential [29], $U_{\text{FENE}}(r) = -0.5kr_0^2 \ln[1-(r/r_0)^2]$ with the molecular spring constant $k = 10\epsilon/\sigma^2$ and the maximum bond length $r_0 = 2\sigma$.

Newton's equations were integrated with the velocity Verlet algorithm with a time step $\delta t = 0.01\tau$, where $\tau = \sigma(m/\epsilon)^{1/2}$ represents the characteristic time scale with bead mass $m=1$ [30]. A Langevin thermostat [31] was used to keep the system at a constant temperature $T = 1.0\epsilon/k_B$ with damping constant $1.0\tau^{-1}$ applied in all directions.

Initially, the system was equilibrated until the steady state was reached ($\approx 10^7$ time steps). We then pulled on the two ends of the polymer chain and obtained the longitudinal force f to keep the ends at a distance $R_{\|}$.

Figure 1 displays a typical number density of beads (squares), denoted by $\rho(r_{\perp})$, for $N=256$ and $D=5$, as a function of $r_{\perp}$, the normal distance from the symmetry axis of the cylinder; this is a result of 5000 different time averages in a long time simulation for $f=0$. [Here and below, all length scales are estimated in units of σ (or a), unless otherwise specified.] The density is normalized so that $\int_0^{R_{\perp}} 2\pi r_{\perp} \rho(r_{\perp}) dr_{\perp} = 1$, where $R_{\perp} \equiv D/2$. Because of the confining wall, $\rho(r_{\perp})$ decays gradually to zero, as $r_{\perp} \to R_{\perp}$. We do not observe any noticeable range of a plateau (for the parameters used), since the corresponding correlation length in bulk [1] is comparable to the blob size D. This implies that the effect of the confining wall propagates up to the center of the cylinder $r_{\perp} \simeq 0$. The slight fluctuations at small $r_{\perp}$ just reflect the cylindrical geometry of the pore: the vanishingly small volume element for $r_{\perp} \to 0$. However, it is not just $\rho(r_{\perp})$ but the combination of $2\pi r_{\perp}\rho(r_{\perp})$, which is relevant in our discussion below [cf. Eq. (7)]—for the latter, the error bars are smaller than the symbols used in Fig. 1. [For this (or similar) reason, we do not include error bars explicitly in Fig. 1 (and in other figures).]

B. Force stretching in a cylindrical pore

We have simulated for a wide range of parameters: $D = 4, 5, \ldots, 14$ and $N = 128, 256, 512$. In Fig. 2(a), we have plotted our simulation results of force vs extension. The force-extension curves (FECs) tend to collapse onto each other for sufficiently large f, where the wall effect becomes minor [32]. Note that for a fixed f the FECs for different values of N converge onto each other. This is consistent with the picture of the confined chain as a linear string of blobs: $R_{\|} \sim N$; the effect of f is to reduce the blob size not the linearity.

Figure 2(b) confirms the previous study [8,13] that the force-relative extension ($\Delta R_{\|} = R_{\|} - R_{\|0}$) curves tend to converge onto one another, when f is rescaled by $D^{0.9}$. The D exponent was chosen by a global fit to the data. This shows that $k_{\text{eff}} \sim N^{-1}D^{-0.9}$. This is a significant deviation from the blob-scaling results [10]. In fact, it has been estimated that the asymptotic limit is reached for $N \gtrsim 10^4$ [13]. Thus the discrepancy can be attributed to finite-size effects. Nevertheless it is evident that k_{eff} increases as D becomes smaller as expected [13].

Our results in Fig. 2 are in excellent agreement with earlier force-extension results [20] despite (slightly) different simulation settings: in the latter, two end beads were confined to piston walls (but otherwise free), while they are free in this study. This is not surprising since the piston-wall boundary condition becomes less important when the chain is stretched with an external force.

C. Release of a force-stretched chain in a cylindrical pore

Using MD simulations, we have also studied the time evolution (relaxation) of a cylindrically confined chain, which is initially stretched beyond its linear regime and then released. To this end, we ignore hydrodynamic effects. (Such chains are said to be in an "immobile" solvent [19].) Then, the relationship between two simulations (stretching and re-

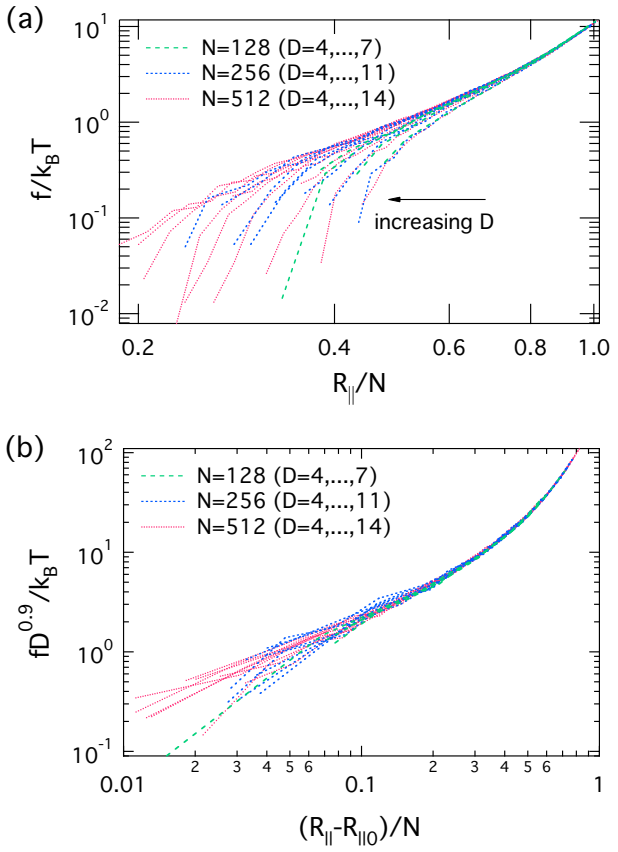

FIG. 2. (Color online) MD simulation results for force-extension curves (FECs). (a) The FEC is sensitive to D for weak-to-moderate deformations; it becomes D independent for sufficiently large f, as it should. On the other hand, the FECs for different choices of N tend to collapse onto each other, when $R_\parallel$ is rescaled by $1/N$. This means linear ordering of the confined chain, i.e., $R_\parallel \sim N$. (b) Rescaled f-extension relations. When f is rescaled by $D^\gamma(\gamma \approx 0.9)$, the FECs converge onto each other; the exponent γ was set by a global fit to the data.

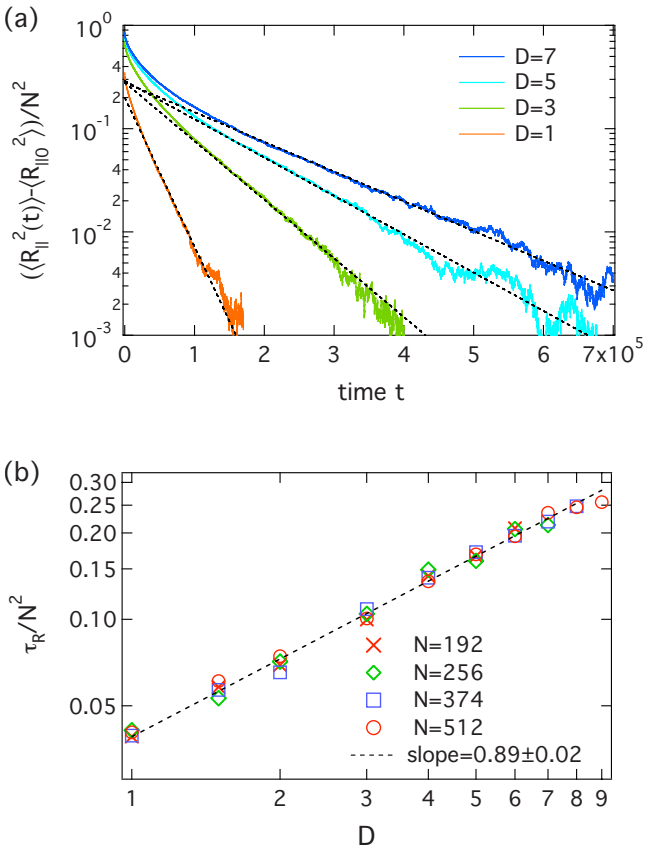

FIG. 3. (Color online) (a) MD simulations of chain relaxation for $N=256$. The time evolution of a polymer, which is initially stretched beyond its linear regime and released, was measured directly using MD simulations. Our results for $(\langle R_\parallel^2(t)\rangle - \langle R_{\parallel 0}^2\rangle)/N^2$ are displayed as a function of time t. Initially, the chain relaxes rapidly and nonexponentially. Chain relaxation crosses over to a single exponential decay: in this regime, $(\langle R_\parallel^2(t)\rangle - \langle R_{\parallel 0}^2\rangle)/N^2 \sim e^{-t/\tau_R}$, where τ_R is the (slower) relaxation time, which governs overall chain relaxation and is the dynamic counterpart of the Hookean response. (b) The slopes of the curves in (a) in the slower relaxation regime are related to the longer relaxation times τ_R. The reduced relaxation time τ_R/N^2 is displayed as a function of D in a log-log plot for a few choices of N. From the slope of the best fit to the data, τ_R is estimated to be $\tau_R \sim N^2 D^\gamma$ with $\gamma \approx 0.89 \pm 0.02$.

laxation) becomes straightforward and the effective spring constant k_{eff} is reciprocally related to relaxation times τ_R as $\tau_R \sim N/k_{\text{eff}}$.

Figure 3(a) shows our simulation results of extension of a stretched chain after release as a function of time. The measured $(\langle R_\parallel^2(t)\rangle - \langle R_{\parallel 0}^2\rangle)/N^2$ is averaged over 800 statistically independent simulations with different realizations of initial conformations, where $\langle \ldots \rangle$ is an ensemble average. Initially, each curve decays rapidly but nonexponentially. It then crosses over to what appears to be a single-exponential decay, i.e., $(\langle R_\parallel^2(t)\rangle - \langle R_{\parallel 0}^2\rangle)/N^2 \sim e^{-t/\tau_R}$, where τ_R is the slope of the curves. This is the dynamic analog of the Hookean regime in the force-extension relation. Obviously the exponential decay represents a slower relaxation compared to the nonexponential decay. In this sense, the overall chain relaxation is mainly governed by the exponential relaxation.

In Fig. 3(b), we see how τ_R/N^2 varies with N and D. For a fixed D, the data for various N values collapse onto each other. The slope of the curves is found to be $\approx 0.89 \pm 0.02$, and we thus find $\tau_R \sim N^2 D^{0.89 \pm 0.02}$. This is indeed consistent with our simulation result for k_{eff} from $\tau_R \sim N/k_{\text{eff}}$. In this analysis, it is assumed that the chain friction is additive (thus overestimated); in reality, however, the friction can be screened by hydrodynamic interactions. For $R_\parallel \simeq R_{\parallel 0}$, i.e., when the chain is in the Hookean regime, the hydrodynamic interaction (HI) can readily be included at the scaling level (see below).

IV. HYDRODYNAMIC INTERACTIONS

At the scaling level, the effect of HI can be considered as renormalizing the chain friction [10]. Let $N_b = N/g \sim N(a/D)^{5/3}$ be the number of blobs and η the solvent viscosity, the friction coefficient of each blob $\xi_{\text{blob}} \sim \eta D$ and thus the chain friction $\xi_{\text{chain}} \sim \eta D \times N_b \sim \eta N a^{5/3} D^{-2/3}$ [10]. On the other hand, $\beta k_{\text{eff}} \sim N_b^{-1} D^{-2} \sim N^{-1} D^{-1/3} a^{-5/3}$ assuming the chain is in the Hookean regime. We then find τ_R

$\sim \xi_{\text{chain}}/k_{\text{eff}} \sim \beta\eta D N_b \times N_b D^2 \sim \beta\eta L^2 a^{4/3} D^{-1/3}$. To summarize, we have

$$\tau_R \sim \beta \begin{cases} \eta L^2 D^{1/3} a^{2/3} & \text{without HI} \\ \eta L^2 D^{-1/3} a^{4/3} & \text{with HI} \end{cases}, \tag{6}$$

where $L=Na$. The hydrodynamic effect is equivalent to replacing the term $(D/a)^{1/3}$ by $(a/D)^{1/3}$, as discussed in Ref. [10].

For finite N, however, the analysis becomes complicated. As shown above and elsewhere [13,8], finite-size (N) effects can persist up to $N \sim 10^4$. Also, the friction renormalization scheme used above ($\xi_{\text{chain}} \sim \eta D \times N_b$) is questionable. Nevertheless, we find an empirical scaling $\beta k_{\text{eff}} \sim N^{-1} D^{-\gamma}$, where the exponent γ deviates from the Hookean scaling result $\gamma = 1/3$ and is nonuniversal in the presence of finite-size effects.

To understand how chain friction is influenced by confinement and finite-size effects, we used our MD results in the theoretical approach to chain diffusion in a pore, proposed by Harden and Doi [9]. The approach is similar, in spirit, to Zimm theory (of an unconfined chain) [2,9] and relies on a set of assumptions and simplifications. First, an implicit (thus continuum) solvent is assumed; the solvent is an incompressible viscous fluid, which influences the dynamics of beads via its viscosity and "no-slip" boundary conditions, i.e., the solvent sticks on each bead and on the confining wall as well. As a result, the HI between beads and the HI between a bead and the confining wall depend on their positions. Perhaps, the most crucial simplification is the preaveraging approximation in which the HI of beads is preaveraged over chain conformations. In principle, the diffusion constant of a confined chain can be obtained without further approximations. For strong confinement or in a narrow capillary ($R_\parallel \gg R_\perp$), however, one can utilize the "ground-state-dominance" approximation, which amounts to keeping the first leading term of the diffusion constant expressed as an infinite series [9].

Let $r_\parallel$ be the longitudinal component of a position vector in a pore and $r_\perp$ a normal distance from the symmetry axis of the pore ($r_\perp \le R_\perp = D/2$); let $\xi^0_{\text{chain}} = \eta N a$, $\rho(r_\perp)$ the normalized monomer density, and $g(k_\parallel)$ the longitudinal structure factor, where $k_\parallel$ is the Fourier conjugate to $r_\parallel$. Then, following Ref. [9], the ground-state-dominance term of ξ_{chain} can be expressed in our notation as

$$\frac{\xi^0_{\text{chain}}}{\xi_{\text{chain}}} \approx \frac{1}{2\pi^2 R_\perp^4} \frac{\alpha_0^2}{J_1^2(\alpha_0)} \left[2\pi \int_0^{R_\perp} dr_\perp r_\perp J_0\left(\frac{\alpha_0 r_\perp}{R_\perp} \right) \rho(r_\perp) \right]^2 \int_{-\infty}^{\infty} dk_\parallel \frac{g(k_\parallel)}{\left[k_\parallel^2 + \left(\frac{\alpha_0}{R_\perp} \right)^2 \right]^2}, \tag{7}$$

where $\alpha_0 \approx 2.405$ is the smallest zero of $J_0(x)$, the zeroth order Bessel function of the first kind. In principle, ξ_{chain} can be written as an infinite series. As argued in Ref. [9], however, the first leading term shown above is a good approximation to the full series, as long as $R_{\parallel 0} \gg R_\perp$.

To analyze Eq. (7), we first invoke some simplification. Perhaps, the most dramatic one is the uniform-density approximation already explored [9], i.e., monomers fill the cylindrical cavity uniformly despite the presence of the confining wall. This simplification leads to $\bar{\rho} = 1/2\pi R_\perp^2$ and $\bar{g}(k_\parallel) = 2N/(R_{\parallel 0} k_\parallel)(1 - \cos k_\parallel R_{\parallel 0})$ [$\approx 2\pi N \delta(k_\parallel)/R_{\parallel 0}$ for $R_\parallel \gg D$] [14]. Accordingly, the blob-scaling result for ξ_{chain} discussed above (in Ref. [10] as well) is reproduced.

In Fig. 4(a), we have plotted ξ_{chain} as a function of D. To this end, we have used explicitly, in Eq. (7), our MD data for $\rho(r_\perp)$ and $g(k_\parallel)$ obtained for $N=256$. [See Fig. 4 for a typical $g(r_\parallel)$, i.e., the inverse Fourier transform of $g(k_\parallel)$.] Our results described by diamonds [top ones (in blue)] in Fig. 4(a) support a simple power law, $\xi_{\text{chain}}/N \sim D^{-0.72}$ represented by the solid line (in blue). The D exponent of ξ_{chain} deviates somewhat from the asymptotic ($N \to \infty$) scaling result $-2/3 \approx -0.67$ [10,9]. When $\bar{g}(k_\parallel)$ was used in place of $g(k_\parallel)$ [diamonds (in cyan)], labeled as "hybrid," the D exponent was found to be -0.71 [the solid line (in cyan)]. The deviation from the full analysis is minor indicating that our simulation data for $g(r_\parallel)$ are well approximated by $\bar{g}(r_\parallel)$. As indicated in Fig. 4(b), the agreement is better for smaller D, as expected on physics grounds; in the extreme case $D \approx a$, the chain resembles a uniform-density rod. On the other hand, when we used $\rho = \bar{\rho}$ and $g(k_\parallel) = \bar{g}(k_\parallel)$ in Eq. (7), we obtained $\xi_{\text{chain}}/N \sim D^{-0.61}$ for $N=256$ [the bottom solid line (in red) in Fig. 4(a)]; in the limit $N \to \infty$, the asymptotic scaling result ($\xi_{\text{chain}}/N \sim D^{-2/3}$) is fully recovered (dotted line) [33].

Why is ξ_{chain}/N not so sensitive to N, while k_{eff} suffers greatly from finite-N effects? First, note that the blob-scaling result for $R_{\parallel 0}$ is easily satisfied for a wide range of N, even though the asymptotic regime for k_{eff} can be reached only if the chain is impossibly long to simulate with the current computational power [13]. In fact, our simulation data for $N=256$ already indicate $R_{\parallel 0} \sim N D^{-0.67}$ (for $4 \le D \le 11$), in excellent agreement with the blob-scaling approach [10,1], while the estimated D exponent of k_{eff} deviates significantly from the scaling exponent. The N dependence enters ξ_{chain} in Eq. (7) mainly via the term $g(k_\parallel)$. Our analysis above (red solid vs black dashed) indicates that $g_\parallel(k_\parallel)$ approaches quickly the asymptotic structure factor $g_\parallel^\infty(k_\parallel) = 2\pi N \delta(k_\parallel)/R_{\parallel 0}$ (data not shown). This demonstrates the insensitivity of ξ_{chain}/N to N (as long as $R_{\parallel 0}/D \gg 1$).

Our results for k_{eff} and ξ_{chain} suggest that $\tau_R = \xi_{\text{chain}}/k_{\text{eff}} \sim \beta\eta N^2 D^{0.17 \pm 0.04}$ [34] for $N=256$. This is in contrast to recent simulation results [11,12], which somehow support the scaling prediction. Caution has to be used here, since the

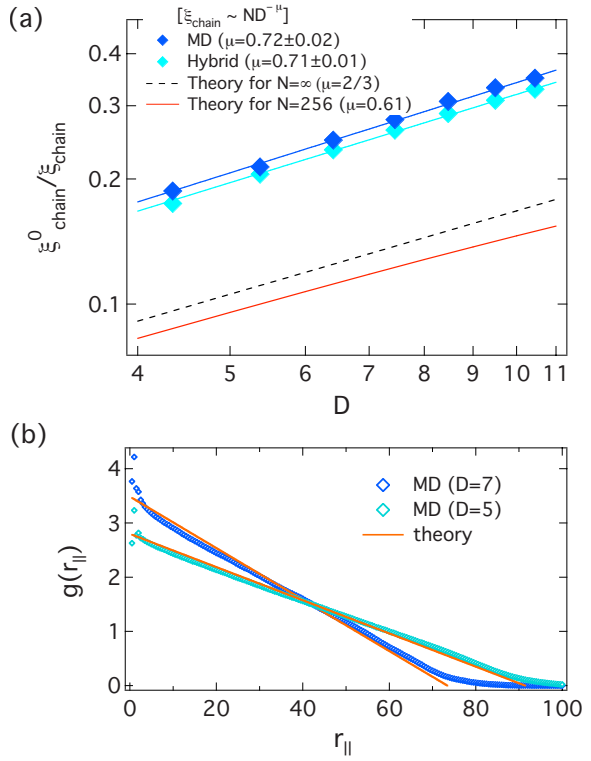

FIG. 4. (Color online) (a) Chain friction versus D for $N=256$. Our results (diamonds) are well described by $\xi_{\text{chain}} \sim ND^{-0.72}$. When $\bar{g}(k_{\|})$ was used in place of $g(k_{\|})$ (labeled as "hybrid"), the D exponent was found to be −0.71. When the monomer density is assumed to be uniform in the pore, the chain friction for $N=256$ is found to be $\xi_{\text{chain}} \sim ND^{-0.61}$ [the bottom solid line (in red)]; as $N \to \infty$, ξ_{chain} converges to what we expect from the blob-scaling approach, i.e., $\xi_{\text{chain}} \sim ND^{-2/3}$. (b) Comparison of our MD simulation result for $g(r_{\|})$ (diamonds) with $\bar{g}(r_{\|})$ [solid lines (in red)], obtained with the assumption of a uniform monomer density, both for $N=256$. Two choices of D were used: $D=5$ and 7 (in units of σ). The overall agreement between simulations and theory is better for the smaller D, as expected; the pronounced discrepancy for sufficiently small $r_{\|}$ arises from monomer correlations within length scales $\lesssim D$, which are suppressed in the uniform density approximation. The discrepancy for large $r_{\|}(r_{\|} \approx R_{\|0})$ originates from end fluctuations. (See Ref. [14] for relevant discussions.)

simulation settings were different in these simulations [11,12] (e.g., nonequilibrium relaxation in [11] and (locally stiff) wormlike chains in a solvent flow in [12]). On the other hand, it is worth noting that our result for k_{eff} is consistent with two other recent results based on flexible-chain models [13,8]; all these support strong finite-size (N) effects on k_{eff} [35]. Naturally, one should expect these effects to persist in the dynamic properties of a confined chain. Furthermore, as explained above, ξ_{chain} (like $R_{\|0}$) is less sensitive to finite-size effects, in the parameter range used in our simulations (also see the endnote [35]). Accordingly, the D dependence of τ_R is expected to deviate significantly from what one may expect from the scaling picture: as a consequence of finite-size effects, k_{eff} increases with decreasing D much more rapidly than in the scaling approaches presented in Sec. II and in Ref. [10]. This effect overcompensates the enhanced friction for smaller D (recall $\xi_{\text{chain}} \sim ND^{-2/3}$ in the scaling limit). This explains the positiveness of the D exponent of τ_R. We expect that the hydrodynamic effect will eventually catch up with the finite-size effect as N increases and become dominant in the scaling limit of $N \to \infty$, as indicated in Eq. (6).

V. CONCLUSION

The emerging conclusion from this work and our recent studies [8] is that a Flory-type approach, if constructed with care, can be used to describe weak-to-moderate chain deformations in the presence of cylindrical confinement. The main advantage is that it offers a simple picture, which is consistent with the blob-scaling approach. For strong stretch outside the Hookean regime, however, both the scaling approach and our Flory approach become inaccurate. In that case, a new length scale, i.e., the tensile blob size (ζ), enters the picture [8]. Because of the subtle interplay between confinement (D) and chain deformations (ζ), the problem of confined polymers in nanopores still defies a complete description (see Ref. [8] for a recent attempt).

On the other hand, our simulations show how chain elasticity and relaxation dynamics are influenced by finite-size effects (which tend to persist up to chain length $N \approx 10^4$). The significant finite-size effects discussed in recent studies [8,13,14] and here are responsible for clear deviations from the scaling predictions of relaxation dynamics in the presence or absence of hydrodynamic interactions [10]. Such considerations will be important in properly interpreting other simulation studies with relatively short chains. However, direct comparison with the recent DNA simulations [12] will be obscured by the aforementioned complexities we ignored in this work. Further consideration along this line will be desirable.

ACKNOWLEDGMENTS

B.Y.H. acknowledges financial support from NSERC (Canada) as well as from the BK 21 Frontier Physics Research Program during his stay at the Department of Physics and Astronomy, Seoul National University, Korea. The work of Y.J. was supported in part by APCTP (the Asia Pacific Center for Theoretical Physics) through the Focus Program on Molecular Dynamics Simulations on Nano/Micro Systems.

[1] P.-G. de Gennes, *Scaling Concepts in Polymer Physics* (Cornell University Press, Ithaca, 1979).

[2] M. Doi and S. F. Edwards, *The Theory of Polymer Dynamics* (Oxford University Press, New York, 1986).

[3] V. Ramakrishnan and P. B. Moore, Curr. Opin. Struct. Biol. **11**, 144 (2001).

[4] S. Jun and B. Mulder, Proc. Natl. Acad. Sci. U.S.A. **103**, 12388 (2006); A. Arnold and S. Jun, Phys. Rev. E **76**, 031901 (2007).

[5] A. Balducci, C.-C. Hsieh, and P. S. Doyle, Phys. Rev. Lett. **99**, 238102 (2007).

[6] J. O. Tegenfeldt *et al.*, Proc. Natl. Acad. Sci. U.S.A. **101**, 10979 (2004).

[7] Confinement has been a major concern in the studies of thin polymer films. In particular it plays a nontrivial role in determining the glass transition temperature, as discussed in the following list of references: K. Dalnoki-Veress, J. A. Forrest, P.-G. de Gennes, and J. R. Dutcher, J. Phys. IV (France) **10**, (P7) 221 (2000); J. A. Torres, P. F. Nealey, and J. J. de Pablo, Phys. Rev. Lett. **85**, 3221 (2000); J. A. Forrest, J. Mattsson, and L. Börjesson, Eur. Phys. J. E **8**, 129 (2002); F. Varnik, J. Baschnagel, K. Binder, and M. Mareschal, *ibid.* **12**, 167 (2003); F. Varnik, J. Baschnagel, and K. Binder, Phys. Rev. E **65**, 021507 (2002); Simone Peter *et al.*, J. Polym. Sci., Part B: Polym. Phys. **44**, 2951 (2006).

[8] S. Jun, D. Thirumalai, and B.-Y. Ha, Phys. Rev. Lett. **101**, 138101 (2008).

[9] J. L. Harden and M. Doi, J. Phys. Chem. **96**, 4046 (1992).

[10] F. Brochard and P.-G. de Gennes, J. Chem. Phys. **67**, 52 (1977).

[11] Y. Sheng and M. Wang, J. Chem. Phys. **114**, 4724 (2001).

[12] R. M. Jendrejack, E. T. Dimalanta, D. C. Schwartz, M. D. Graham, and J. J. de Pablo, Phys. Rev. Lett. **91**, 038102 (2003).

[13] A. Arnold, B. Borzorgui, D. Frenkel, B.-Y. Ha, and S. Jun, J. Chem. Phys. **127**, 164903 (2007).

[14] K. Kremer and K. Binder, J. Chem. Phys. **81**, 6381 (1984).

[15] P. J. Flory, *Principles of Polymer Chemistry* (Cornell University Press, Ithaca, NY, 1953).

[16] More systematically, one can calculate the free energy $\mathcal{F}$ of a self-avoiding chain using a relatively simple trial monomer distribution. The Flory approach is equivalent to choose R as a variational parameter and use a Gaussian distribution of R, as for an ideal chain [see, for example, J. des Cloizeaux and G. Jannink, *Polymers in Solution: Their Modeling and Structure* (Oxford University Press, New York, 1990)].

[17] P. J. Flory and W. R. Krigbaum, J. Chem. Phys. **18**, 1086 (1950).

[18] A. Y. Grosberg, P. G. Khalatur, and A. R. Khokhlov, Makromol. Chem., Rapid. Commun. **3**, 709 (1982).

[19] A. R. Khokhlov and A. Y. Grosberg, *Statistical Physics of Macromolecules* (AIP Press, New York, 1994).

[20] S. Jun, A. Arnold, and B.-Y. Ha, Phys. Rev. Lett. **98**, 128303 (2007).

[21] The Flory free energy $\mathcal{F}$ here includes terms describing chain elasticity and two-body volume interactions, but not any term, which is linear with N.

[22] D. W. Schaefer, J. F. Joanny, and P. Pincus, Macromolecules **13**, 1280 (1980).

[23] H. Nakanishi, J. Phys. (France) **48**, 979 (1987).

[24] T. A. Vilgis, Phys. Rep. **336**, 167 (2000).

[25] F. Brochard-Wyart and E. Raphael, Macromolecules **23**, 2276 (1990).

[26] M. Rubinstein and R. Colby, *Polymer Physics* (Oxford University Press, Oxford, UK, 2003).

[27] We also note that this compactness of the 1-d case agrees with our mean-field picture [cf. Eq. (4)]. To see this, we calculate the relative end-to-end distance fluctuation of the chain using Eq. (4), $\delta R_{\|}/R_{\|0} \sim k_{\mathrm{eff}}^{-1/2} R_{\|0}^{-1} \sim (D/a)^{11/6} N^{-1/2}$. (This is consistent with the scaling analysis [10].) Thus, for $(D/a)^{11/3} \ll N$, the overall chain fluctuations become negligible. On the other hand, the noncompactness of higher spatial dimensions makes the effect of fluctuations more serious in that any mean-field approach is less reliable. For instance, Eq. (1) for $d=3$ erroneously implies that $\delta R/R_F \sim N^{-1/10} \to 0$ for large N. The correct relation is $\delta R \sim R_F$—the chain size in this compact noncompact case is set by the end fluctuation. We believe Eq. (5) suffers from a similar inconsistency.

[28] J. D. Weeks, D. Chandler, and H. C. Andersen, J. Chem. Phys. **54**, 5237 (1971).

[29] K. Kremer and G. S. Grest, J. Chem. Phys. **92**, 5057 (1990).

[30] M. P. Allen and D. J. Tildesley, *Computer Simulation of Liquids* (Clarendon, Oxford, 1987).

[31] G. S. Grest and K. Kremer, Phys. Rev. A **33**, 3628 (1986).

[32] This should be, however, understood with caution: near the full stretch, the FECs are sensitive to intermolecular interactions that hold adjacent monomers together and hence are model dependent. Nevertheless, note that the FECs eventually become D independent.

[33] In our analysis with a constant ρ, we combined the scaling result for $R_{\|0}(R_{\|0} \approx 1.1 \times D^{-2/3} N)$ with $\bar{g}(k_{\|})$; to this end, the numerical prefactor was chosen to ensure the best fit to our simulation data for $R_{\|0}$ (when $N=256$ was used). In our "hybrid" analysis with numerically determined $\rho(r_{\perp})$ (diamonds in cyan in Fig. 4), however, both the numerical prefactor and the D exponent were determined from the data. As described later in the main text, the resulting D exponent (≈ 0.67) is in excellent agreement with the scaling result. Thus the discrepancy between diamonds in cyan (as well as in blue) and the red line mainly comes from the difference in the functional behavior of $\rho(r_{\perp})$.

[34] Note that ξ_{chain} given in Eq. (7) is the friction for diffusion of a confined chain in a narrow capillary, more precisely the friction for longitudinal diffusion of its center of mass. [The wall effect is through the no-slip boundary condition mentioned above Eq. (7).] Imagine that the center of mass, denoted as R_{CM}, is subject to a constant external force in the longitudinal direction, f_{ext}. Obviously, the force balance leads to $f_{\mathrm{ext}} = \xi_{\mathrm{chain}} dR_{\mathrm{CM}}/dt$, if the inertia term is ignored. One can argue that this is also the friction for the slowest-relaxation mode of the confined chain ($\propto \tau_R$). The only difference is that the force experienced by the slowest mode is a harmonic force (see Ref. [10]). In the case of a Rouse chain (an ideal noninteracting chain), the friction coefficient of chain diffusion can readily be shown to coincide with that for the slowest-relaxation mode (see for instance Ref. [2]).

[35] What remains unclear is why the scaling regime for k_{eff} is reached only slowly. While a complete picture is still elusive, we believe that this can be attributed to the fact that k_{eff} is related to the variation in free energy with $R_{\|}$ around its mini-

mum. The blob-scaling picture hinges on the (hidden) assumption that each blob deforms independently of each other; thus the free energy cost per each blob can be obtained accordingly. It is conceivable that this assumption works better for larger N_b (No. of blobs) and D; at the opposite extreme limit of $D \approx a$, blob deformations are expected to be strongly correlated. This may explain the discrepancy and the sensitivity of k_{eff} to finite-size effects. On the other hand, such quantities as $R_{\parallel 0}$ and $g_{\parallel}(R_{\parallel})$ are essentially determined by free-energy minima, not variations; they are expected to enter the scaling regime more easily, as demonstrated in this work (see also Ref. [13] for relevant discussions).